Nickel-catalyzed coordination polymerization-induced self-assembly of helical poly(aryl isocyanide)s

Jimaja, Setuhn; Varlas, Spyridon; Xie, Yujie; Foster, Jeff; Taton, Daniel; Dove, Andrew; O'Reilly, Rachel

DOI:
10.1021/acsmacrolett.9b00972

Nickel-catalyzed coordination polymerization-induced self-assembly of helical poly(arylisocyanide)s

Sètuhn Jimaja,[†,‡,§] Spyridon Varlas,[‡] Yujie Xie,[†,‡] Jeffrey C. Foster,[‡] Daniel Taton,[§] Andrew P. Dove[‡*] and Rachel K. O'Reilly[‡*]

[†]Department of Chemistry, University of Warwick, Coventry, CV4 7AL, United Kingdom

[‡]School of Chemistry, University of Birmingham, Edgbaston, B15 2TT, United Kingdom

[§]Laboratoire de Chimie des Polymères Organiques, Université de Bordeaux / CNRS École Nationale Supérieure de Chimie, de Biologie & de Physique, 33607 Pessac Cedex, France

ABSTRACT: The interest in helix-containing nanostructures is currently growing as a consequence of their potential applications in areas such as nanomedicine, nanomaterial design, chiral recognition and asymmetric catalysis. Herein, we present a facile and tunable one-pot methodology to achieve chiral nano-objects. The nickel-catalyzed coordination polymerization-induced self-assembly (NiCCo-PISA) of helical poly(arylisocyanide) amphiphilic diblock copolymers was realized and allowed access to various nano-object morphologies (spheres, worm-like micelles and polymersomes). Helicity of the core block was confirmed *via* circular dichroism (CD) spectroscopy for all morphologies, proving their chiral nature. Small molecule uptake by the spherical nanoparticles was investigated by encapsulating Nile Red into the core of the spheres and subsequent transfer into aqueous media. The presence of a CD signal for the otherwise CD-inactive dye proved the chiral induction effect of the nano-objects' helical core. This demonstrates the potential of NiCCo-PISA to prepare nanoparticles for applications in nanomaterials, catalysis and recognition.

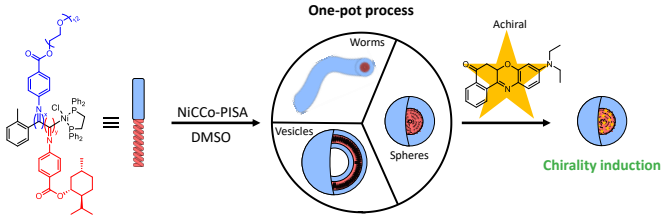

Helices and helical assemblies are important structures in bio-macromolecules that are employed in many roles in nature from providing structure in the case of collagen to storing information (*i.e.*, DNA) to the many purposes the α-helix has in protein assembly and function.[1] One of the most remarkable attributes of the helical architecture is its inherent chirality – right- and left-handed helices are the mirror image of one another, but are not superimposable. This chirality gives the helix an obvious role in recognition, which is well demonstrated by the α-helices present in the Zinc finger motif for its binding to DNA double helix or proteins.[2-4]

Taking the polyvalence of the helical structure as inspiration, chemists have applied synthetic helices to different areas[5-7] such as nanomaterials,[8-10] chiral recognition,[11-14] and catalysis.[15-19] In the field of nanomaterials, using nature's building blocks, Lecommandoux and coworkers investigated the synthesis and self-assembly of polypeptide-based diblock copolymers into different nanostructures and studied their possible application as stimuli-responsive materials.[20-22] To replicate the properties of cell penetrating peptides (CPP), which have excellent membrane permeability in part as a consequence of their helical shape[23], Wu and coworkers reported that rapid cellular internalization was observed with PEGylated left-handed helical poly(phenyl isocyanide) corona micelles.[24, 25] However, such assemblies are usually prepared by methods that are time- and resource-consuming and give solutions with a relatively low content of polymer.

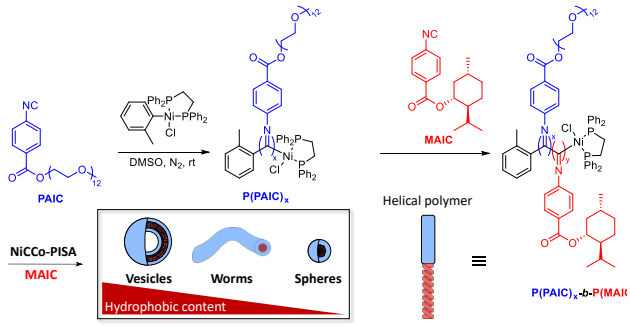

Scheme 1: Synthetic route followed for the preparation *via* NiCCo-PISA of **P(PAIC)$_x$-*b*-P(MAIC)$_y$** diblock copolymer nanostructures.

An alternative route to prepare nanostructures is polymerization-induced self-assembly (PISA), which is an efficient approach to achieve nanostructures with different morphologies at high solids concentrations (up to 50 wt%) using simple experimental procedures.[26-31] PISA is usually conducted by radical polymerization techniques[32-39] and while metal-catalyzed coordination polymerization methodologies for PISA, for instance ring-opening metathesis-mediated PISA (ROMPISA),[40-43] provide entirely new possible backbone and side-chain chemistry, such methods have yet to be fully explored to the same degree as their radical counterparts.

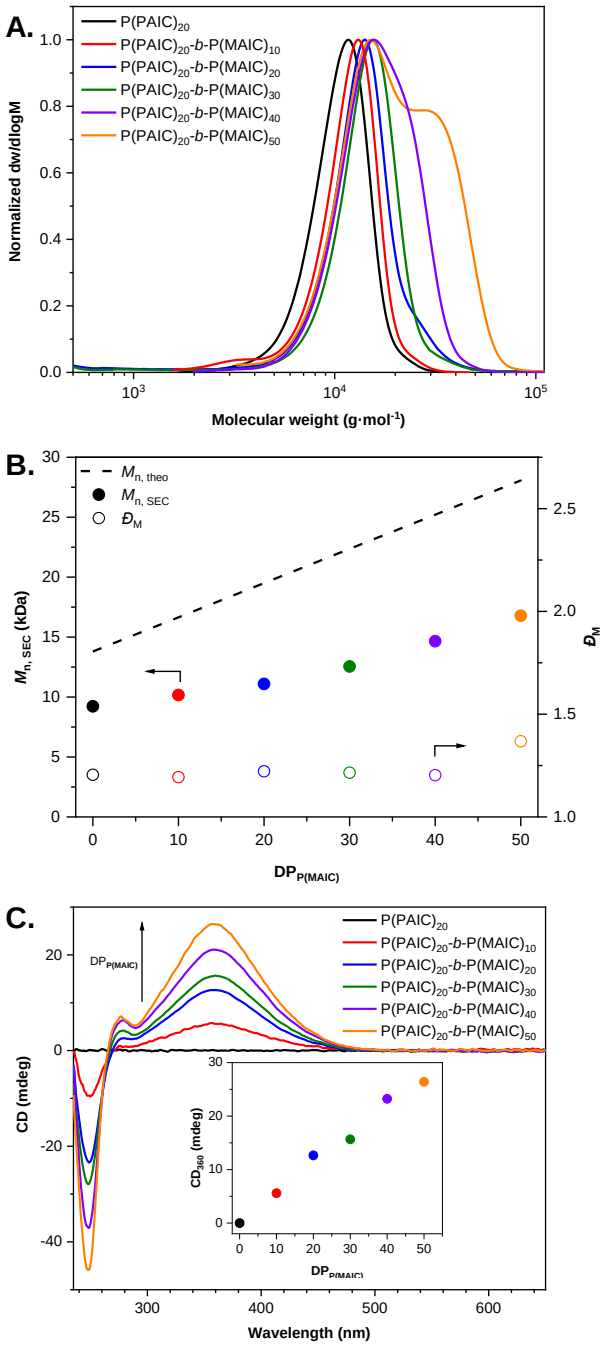

Figure 1: SEC and CD analysis of **P(PAIC)$_{20}$-*b*-P(MAIC)$_y$** diblock copolymers. Polymerizations were conducted at r.t. in DMSO at a solids weight content of 5 wt%. (A) Normalized SEC RI molecular weight distributions (THF + 2% v/v NEt_3, 40 °C, PS standards) for **P(PAIC)$_{20}$** macroinitiator and **P(PAIC)$_{20}$-*b*-P(MAIC)$_y$** block-copolymers. (B) Evolution of $M_{n,\,SEC}$ (filled circle) and $Đ_M$ (hollow circle) values measured by SEC as a function of targeted $DP_{P(MAIC)}$. The $M_{n,\,theo}$ (dashed line) calculated from the monomer molecular weight and polymerization conversion is displayed as reference. (C) CD (THF, 0.5 mg·mL^{-1}) spectra. *Inset:* CD signal at λ = 360 nm plotted *vs* the $DP_{P(MAIC)}$.

PISA offers the advantage of encapsulating small molecules *in situ* during polymerization.[44, 45] Since NiCCo-PISA occurs at room temperature, there is little risk of damaging thermolabile compounds such as drugs or enzymes. In this contribution, we report the *in situ* synthesis and self-assembly of helical polyisocyanides into different nanostructures *via* NiCCo-PISA and their chiral induction effect on an encapsulated achiral dye (Nile Red). We anticipate that such nanostructures will be useful in a variety of applications from helix-containing delivery systems to chiral recognition or catalysis of asymmetric reactions where the chiral core could be leveraged.

Table 1: Characterization of synthesized **P(PAIC)$_x$-*b*-P(MAIC)$_y$** diblock copolymers.

Sample[a]	$M_{n,\,theo}$ (kDa)[b]	$M_{n,\,SEC}$ (kDa)[c]	$Đ_M$[c]	CD_{360}[d] (mdeg)
P(PAIC)$_{10}$	6.9	6.5	1.24	0
P(PAIC)$_{10}$-*b*-P(MAIC)$_{10}$	9.8	7.3	1.25	11
P(PAIC)$_{10}$-*b*-P(MAIC)$_{20}$	12.6	8.5	1.17	14
P(PAIC)$_{10}$-*b*-P(MAIC)$_{30}$	15.5	10.1	1.25	22
P(PAIC)$_{10}$-*b*-P(MAIC)$_{40}$	18.3	11.6	1.42	23
P(PAIC)$_{10}$-*b*-P(MAIC)$_{50}$	21.1	13.8	1.58	27
P(PAIC)$_{20}$	13.8	9.2	1.20	0
P(PAIC)$_{20}$-*b*-P(MAIC)$_{10}$	16.7	10.2	1.19	6
P(PAIC)$_{20}$-*b*-P(MAIC)$_{20}$	19.5	11.1	1.22	13
P(PAIC)$_{20}$-*b*-P(MAIC)$_{30}$	22.4	12.5	1.21	16
P(PAIC)$_{20}$-*b*-P(MAIC)$_{40}$	25.2	14.7	1.20	23
P(PAIC)$_{20}$-*b*-P(MAIC)$_{50}$	28.1	16.8	1.37	26
P(PAIC)$_{30}$	20.7	12.8	1.13	0
P(PAIC)$_{30}$-*b*-P(MAIC)$_{10}$	23.6	15.7	1.28	5
P(PAIC)$_{30}$-*b*-P(MAIC)$_{20}$	26.4	16.8	1.31	10
P(PAIC)$_{30}$-*b*-P(MAIC)$_{30}$	29.3	18.0	1.35	12
P(PAIC)$_{30}$-*b*-P(MAIC)$_{40}$	32.1	18.4	1.45	19
P(PAIC)$_{30}$-*b*-P(MAIC)$_{50}$	35.0	18.5	1.53	21
P(MAIC)$_{50}$	14.3	7.1	1.16	38

[a]All conversions were > 99%, as determined by ^{1}H NMR spectroscopy in $CDCl_3$.
[b]Calculated from conversion using the monomer's MW and feed ratio.
[c]Determined by SEC (THF + 2% v/v NEt_3, 40 °C, PS standards).
[d]CD signal at λ = 360 nm.

This account expands the library of methodologies and monomers accessible by PISA by introducing the nickel-catalyzed coordination polymerization of arylisocyanides (NiCCo-PISA). Furthermore, to the best of our knowledge, this work represents the first report of PISA conducted with helical polymers.

The common methodology to conduct dispersion PISA is through the chain-extension of a solvophilic block with a solvent-miscible monomer whose corresponding homopolymer is solvophobic. The growing polymer block gradually becomes insoluble in the reaction media, forming an amphiphilic diblock copolymer that self-assembles *in situ*.[27] In our early attempts to synthesize poly(isocyanide)s with chiral L-menthol side-chains, we observed precipitation of the growing polymer in DMSO during polymerization. Thus, we reasoned that menthyl-ester arylisocyanide (**MAIC**)[46, 47] could be utilized as the core-forming monomer in PISA formulations (**Scheme 1**). Toward this end, a DMSO-soluble PEG-ester aryl isocyanide (**PAIC**) monomer was synthesized as the corona block. A PEG side-chain was chosen because of the expected solubility in both water and DMSO of the monomer and homopolymer as well as its known biocompatibility. Both **PAIC** and **MAIC** were homopolymerized *via* a coordination polymerization catalyzed by *o*-

Tol(dppe)NiCl[48] in DMSO and THF, respectively. Excellent control over the polymerization process was observed in both cases, and polymers were obtained with moderate dispersities (**Table S2**).

NiCCo-PISA was conducted by the *in-situ* chain-extension of a **P(PAIC)$_x$** macroinitiator using **MAIC** in DMSO, yielding diblock copolymers **P(PAIC)$_x$-*b*-P(MAIC)$_y$** (**Figure 1A**). The control over the polymerization was verified by targeting different degrees of polymerization (DPs) of both the solvophilic and solvophobic blocks and constructing M_n *vs* DP$_{P(MAIC)}$ plots (**Figure 1B** and **Figure S30-32**). A linear relationship between targeted DP and molecular weight indicated the polymerization process was controlled (**Table 1**). However, when targeting high DP$_{P(MAIC)}$ high molecular weight shoulders are observed.. When the chain-extension of the macroinitiator is conducted in a good solvent, namely THF, no shoulder is observed, suggesting that the apparition of that second population most likely originates from the PISA process itself. The measured molecular weight evolution was similar to what has been reported previously.[48]

Polyisocyanides are inherently helical in nature, and this helicity can be detected by circular dichroism (CD) spectroscopy. Moreover, these helices are static, meaning that changes in helicity at room temperature are seldom observed.[6] However, in the absence of a driving force to influence the equilibrium occurring during polymerization between both screw-senses, they are present in equal quantities and the overall CD signal is null as in the case of the homopolymer **P(PAIC)**. On the contrary, in **P(MAIC)**, the chiral moiety on the side chain kinetically favors one of the helix screw-senses and this excess can be measured by CD (**Figure S27**).[47] To determine whether the diblock copolymers obtained from NiCCo-PISA exhibited helicity, **P(PAIC)$_x$-*b*-P(MAIC)$_y$** copolymers of different block ratios were analyzed by CD spectroscopy after dissolution in THF to circumvent the possible interferences emerging from light-scattering by the nano-objects (**Figure 1C**). While the **P(PAIC)** homopolymers did not display any signal, the diblock copolymers showed a clear signal at 360 nm, consistent with previous literature reports.[46-48] By comparing the change in the intensity of this signal for the different hydrophobic block lengths, a linear increase of signal response with the DP$_{P(MAIC)}$ was observed, confirming the helical nature of the nanostructures' core for all the DPs and ratios studied (**Table 1**). Importantly, as a consequence of the static nature of the helix, the CD spectrum of the copolymer unimers dissolved in THF is expected be similar to that of the nanoparticles in DMSO. The slope of the CD *vs* DP$_{P(MAIC)}$ plot became more gradual as the **PAIC** content was increased, concurrent with the increased content of opposite screw-sense helices present in the **P(PAIC)** block (**Figure S33**).

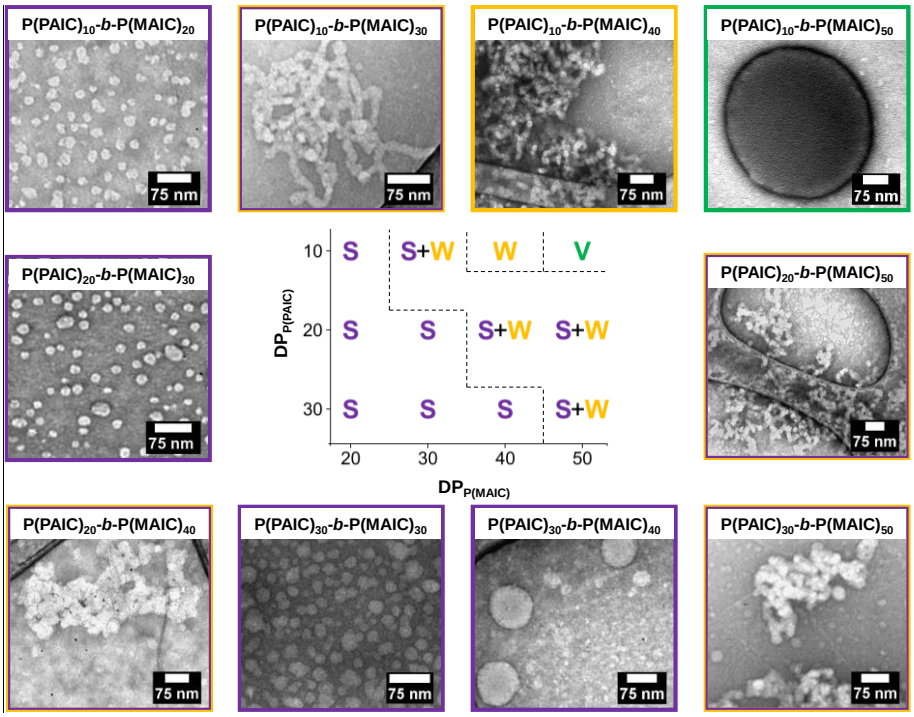

Figure 2: Phase diagram for **P(PAIC)$_x$-*b*-P(MAIC)$_y$** diblock copolymer nano-objects prepared *via* NiCCo-PISA (5 wt% solids content) by varying the DP$_{P(PAIC)}$ and DP$_{P(MAIC)}$, along with representative dry-state TEM images of different formulations.

As a consequence of the insolubility of **P(MAIC)** in DMSO, chain-extension of a **P(PAIC)** macroinitiator with **MAIC** led to the formation of self-assembled nanostructures. Dynamic light scattering (DLS) was used to measure the size of the nano-objects in the various block copolymer solutions targeting different DPs. For the **P(PAIC)$_x$-*b*-P(MAIC)$_{20}$** series, single populations of nano-objects were observed, with sizes ranging from 16 – 25 nm depending on DP$_{P(PAIC)}$. As the targeted DP$_{P(MAIC)}$ was increased, multiple nano-object populations were detected, consistent with the evolution of mixed morphologies possibly containing both spherical and worm-like micelles. At high DP$_{P(MAIC)}$, primarily mixed morphologies were obtained with the exception of **P(PAIC)$_{10}$-*b*-(PMAIC)$_{50}$**, which exhibited a single population of particles with D_H = 630 nm.

Transmission electron microscopy (TEM) was employed to determine the obtained morphologies – in this case spheres, worm-like micelles and polymersomes were achieved. (**Figure 2**). In brief, the $DP_{P(MAIC)}$ = 20 series consisted of spherical micelles with D_{TEM} = 18, 17, and 21 nm for **P(PAIC)$_{10}$-*b*-(PMAIC)$_{20}$**, **P(PAIC)$_{20}$-*b*-(PMAIC)$_{20}$**, and **P(PAIC)$_{30}$-*b*-(PMAIC)$_{20}$**, respectively, in good agreement with the data obtained from DLS (**Table S4**). Mixed morphologies containing both spherical and worm-like micelles occupied an intermediate DP range in the phase space. For the **P(PAIC)$_{10}$-*b*-P(MAIC)$_{40}$** sample, a pure phase of worm-like micelles was apparent in the TEM images. Upon further increasing the $DP_{P(MAIC)}$ to 50, polymersomes were obtained with D_{TEM} = 490 nm. The observed difference in diameter between DLS and TEM analysis is most possibly attributed to drying effects during the sample preparation process prior to TEM imaging that would induce shrinkage of the particle. This polymersome morphology was confirmed by static light scattering (SLS) where the Debye method was employed to calculate an aggregation number of 3.68×10^3 and a R_g/R_H of 1.04, confirming the hollow sphere nature of the **P(PAIC)$_{10}$-*b*-P(MAIC)$_{50}$** nanoparticles (**Figure S46 and Table S5**). Overall, decreasing the length of the **P(PAIC)** stabilizer block or increasing the length of the **P(MAIC)** core block resulted in the formation of higher-order morphologies such as worm-like micelles or polymersomes. Importantly, these higher-order morphologies were also demonstrated to retain their core helicity, extending the breadth of possible nanostructures that can be synthesized in one step using a simple PISA methodology. In order to use our polymeric system in a biologically relevant environment, the spherical micelle samples were transferred into water by dialysis. An increase of the micelle diameter from 25 to 60 nm was observed by DLS following the dialysis step; however, no change in size over > 4 weeks indicated the particles were colloidally stable (**Figure S48**). The capability to obtain stable, helices-containing micelles in aqueous media expanded the window of potential applications, prompting us to explore the possibility of inducing chirality in small molecules *via* encapsulation within the nanoparticle cores. To assess the capability of the spherical micelles to encapsulate hydrophobic species, NiCCo-PISA targeting **P(PAIC)$_{20}$-*b*-P(MAIC)$_{30}$** was conducted in a solution containing 1 wt% - relative to the polymer content - of the lipophilic dye Nile Red (NR). We expected the dye to be taken up into the hydrophobic nanoparticle cores during the PISA process and the resulting dialyzed solution to be fluorescent. After dialysis, the aqueous solution was centrifuged and the supernatant was filtered to remove un-encapsulated NR. The resulting solution retained fluorescence, and further analysis by spectrophotometry confirmed the presence of NR within the nanoparticles (**Figure S49**). As a consequence of the dye's solvatochromic nature, a shift from the maximum emission of NR in water (660 nm) to the encapsulated solution (635 nm) was observed, proving effective encapsulation of NR in the nanostructure cores and the lack of signal at 660 nm confirmed the successful removal of un-encapsulated NR (**Figure S49**). This uptake experiment was repeated with different initial concentrations of NR (0.5, 2, 5, 10 and 15 wt%) to determine the maximum loading. Aliquots from each NiCCo-PISA were taken after purification and freeze-dried. The resulting residues were dissolved in THF and analyzed by UV/Vis spectroscopy (**Figure 3A**). Using this formulation and an initial concentration of NR of 5wt%, the encapsulation and maximum loading were calculated, obtaining 42% and 2.3 wt% respectively. (**Table S8**).

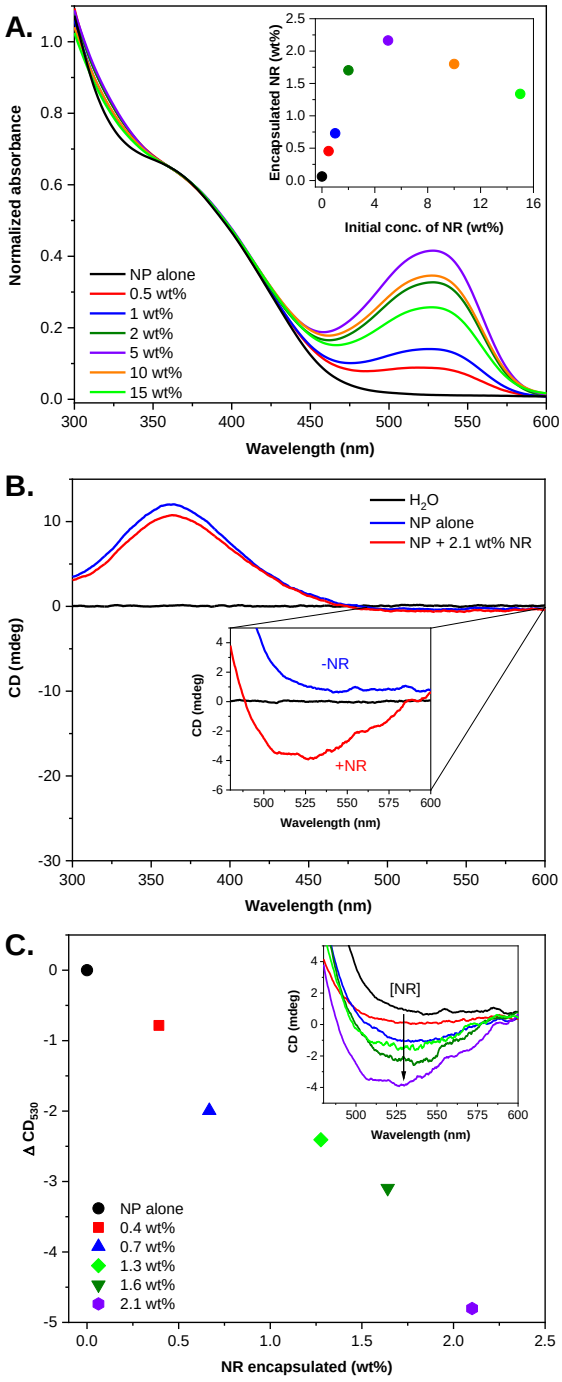

Figure 3: NiCCo-PISA of **P(PAIC)$_{20}$-*b*-P(MAIC)$_{30}$** conducted in DMSO in the presence of NR. (A) UV/Vis (THF, 1 mg·mL^{-1}) spectra of the copolymer and dye at different initial NR concentration. *Inset:* Concentration of encapsulated NR depending on the initial NR concentration. (B) CD (H_2O) absorption spectra of the nanoparticle (NP) (blue) and NR-loaded NP (red). *Inset:* Close-up on the NR absorption region at a higher concentration to allow detection of the signal. (C) Linear dependence of the CD response to the loading of NR in the NPs. *Inset*: CD (H_2O) absorption spectra of the NiCCo-PISA solutions with different NR loadings.

The helical core of the **P(PAIC)$_{20}$-*b*-P(MAIC)$_{30}$** spherical micelles was hypothesized to induce a similar effect on the encapsulated NR arising solely from its chiral-core environment without supramolecular helicity. Achiral (*i.e.* CD-inactive) dyes

confined within helical supramolecular assemblies have been shown to exhibit CD activity by chirality transfer from the helical environment.[49-52] To verify this hypothesis, the CD measurement of the dye-loaded spherical micelles showed a signal in the region corresponding to NR (**Figure 3B**), providing evidence that the chiral nanoparticle environment influenced the absorption of a dye that was otherwise CD-inactive. This chiral induction was shown to evolve linearly with the content of NR in the nano-objects, demonstrating the CD signal originated from the encapsulated dye (**Figure 3C**). The chiral-induction effect of the core's helical environment unveil the potential of these nano-objects in applications such as chiral recognition and asymmetric catalysis.

To conclude, we report a new polymerization technique applied to PISA that produces nanoparticles with helical blocks, and its successful utilization to achieve nano-objects with common morphologies – spheres, worm-like micelles and polymersomes – by varying the DP of the corona- or the core-forming blocks. This relation was presented as a phase diagram demonstrating that higher overall hydrophobic content yielded higher-order morphologies. Preservation of the helicity of the core polymer for all the morphologies during the self-assembly process was confirmed by CD. Encapsulation of NR was performed effectively with **P(PAIC)$_{20}$-*b*-P(MAIC)$_{30}$** copolymer for a range of dye concentrations and after transfer into water the helical core was shown by CD spectroscopy to have a chiral-induction effect. Overall, the reported methodology and the resulting nano-objects could find applications in areas such as nanomedicine, chiral separation, and enantioselective catalysis.

ASSOCIATED CONTENT

The Supporting Information is available free of charge on the ACS Publications website at DOI: 10.1021/acsmacrolett.xxxxxxx.
Additional characterization results including materials, experimental procedures, characterization techniques, and additional data (SEC, NMR, TEM, DLS, SLS, UV/Vis, FT-IR, CD, HR-MS, and fluorescence spectra).

AUTHOR INFORMATION

Corresponding Authors

* Email: a.dove@bham.ac.uk
* Email: r.oreilly@bham.ac.uk

ORCID

Sètuhn Jimaja: 0000-0001-6136-0550
Spyridon Varlas: 0000-0002-4171-7572
Yujie Xie: 0000-0002-6024-7019
Jeffrey Foster: 0000-0002-1043-7172
Daniel Taton: 0000-0002-8539-4963
Andrew Dove: 0000-0001-8208-9309
Rachel O'Reilly: 0000-0002-1043-7172

Authors Contribution

The manuscript was written through contributions of all authors. All authors have given approval to the final version of the manuscript.

Notes

The authors declare no competing financial interest.

ACKNOWLEDGMENT

This work was supported by the European Union (SUSPOL-EJD 642671), ERC (grant number 615142), EPSRC and the University of Birmingham. Dr R. Keogh (University of Birmingham) is thanked for SLS assistance.

REFERENCES

(1) Pelley, J. W., 3 - Protein Structure and Function. In *Elsevier's Integrated Biochemistry*, Pelley, J. W., Ed. Mosby: Philadelphia, 2007; 19-28.
(2) Pavletich, N. P.; Pabo, C. O., Zinc finger-DNA recognition: crystal structure of a Zif268-DNA complex at 2.1 Å. *Science*, **1991,** *252*, 809-817.
(3) Desjarlais, J. R.; Berg, J. M., Toward rules relating zinc finger protein sequences and DNA binding site preferences. *Proceedings of the National Academy of Sciences* **1992,** *89*, 7345-7349.
(4) Gamsjaeger, R.; Liew, C. K.; Loughlin, F. E.; Crossley, M.; Mackay, J. P., Sticky fingers: zinc-fingers as protein-recognition motifs. *Trends Biochem. Sci.* **2007,** *32*, 63-70.
(5) Nakano, T.; Okamoto, Y., Synthetic Helical Polymers: Conformation and Function. *Chem. Rev.* **2001,** *101*, 4013-4038.
(6) Yashima, E.; Maeda, K.; Iida, H.; Furusho, Y.; Nagai, K., Helical Polymers: Synthesis, Structures, and Functions. *Chem. Rev.* **2009,** *109*, 6102-6211.
(7) Yashima, E.; Ousaka, N.; Taura, D.; Shimomura, K.; Ikai, T.; Maeda, K., Supramolecular Helical Systems: Helical Assemblies of Small Molecules, Foldamers, and Polymers with Chiral Amplification and Their Functions. *Chem. Rev.* **2016,** *116*, 13752-13990.
(8) Kouwer, P. H. J.; Koepf, M.; Le Sage, V. A. A.; Jaspers, M.; van Buul, A. M.; Eksteen-Akeroyd, Z. H.; Woltinge, T.; Schwartz, E.; Kitto, H. J.; Hoogenboom, R.; Picken, S. J.; Nolte, R. J. M.; Mendes, E.; Rowan, A. E., Responsive biomimetic networks from polyisocyanopeptide hydrogels. *Nature* **2013,** *493*, 651-655.
(9) Jaspers, M.; Pape, A. C. H.; Voets, I. K.; Rowan, A. E.; Portale, G.; Kouwer, P. H. J., Bundle Formation in Biomimetic Hydrogels. *Biomacromolecules* **2016,** *17*, 2642-2649.
(10) Zimoch, J.; Padial, J. S.; Klar, A. S.; Vallmajo-Martin, Q.; Meuli, M.; Biedermann, T.; Wilson, C. J.; Rowan, A.; Reichmann, E., Polyisocyanopeptide hydrogels: a novel thermo-responsive hydrogel supporting pre-vascularization and the development of organotypic structures. *Acta Biomaterialia* **2018,** *70*, 129-139.
(11) Miyabe, T.; Iida, H.; Ohnishi, A.; Yashima, E., Enantioseparation on poly(phenyl isocyanide)s with macromolecular helicity memory as chiral stationary phases for HPLC. *Chem. Sci.* **2012,** *3*, 863-867.
(12) Numata, M.; Kinoshita, D.; Hirose, N.; Kozawa, T.; Tamiaki, H., Orthogonal Polymer Recognition Based on Semiartificial Helical Polysaccharide. *Chem. Lett.* **2013,** *42*, 266-268.
(13) Liu, N.; Ma, C.-H.; Sun, R.-W.; Huang, J.; Li, C.; Wu, Z.-Q., Facile Synthesis and Chiral Recognition of Block and Star Copolymers Containing Stereoregular

Helical Poly(phenyl isocyanide) and Polyethylene Glycol Blocks. *Polym. Chem.* **2017,** *8*, 2152-2163.
(14) Wang, Q.; Chu, B.-F.; Chu, J.-H.; Liu, N.; Wu, Z.-Q., Facile Synthesis of Optically Active and Thermoresponsive Star Block Copolymers Carrying Helical Polyisocyanide Arms and Their Thermo-Triggered Chiral Resolution Ability. *ACS Macro Letters* **2018,** *7*, 127-131.
(15) Reggelin, M.; Doerr, S.; Klussmann, M.; Schultz, M.; Holbach, M., Helically chiral polymers: A class of ligands for asymmetric catalysis. *PNAS* **2004,** *101*, 5461-5466.
(16) Bécart, D.; Diemer, V.; Salaün, A.; Oiarbide, M.; Nelli, Y. R.; Kauffmann, B.; Fischer, L.; Palomo, C.; Guichard, G., Helical Oligourea Foldamers as Powerful Hydrogen Bonding Catalysts for Enantioselective C–C Bond-Forming Reactions. *J. Am. Chem. Soc.* **2017,** *139*, 12524-12532.
(17) Yamamoto, T.; Murakami, R.; Suginome, M., Single-Handed Helical Poly(quinoxaline-2,3-diyl)s Bearing Achiral 4-Aminopyrid-3-yl Pendants as Highly Enantioselective, Reusable Chiral Nucleophilic Organocatalysts in the Steglich Reaction. *J. Am. Chem. Soc.* **2017,** *139*, 2557-2560.
(18) Zhao, B.; Deng, J. R.; Deng, J. P., Optically Active Helical Polyacetylene Self-Assembled into Chiral Micelles Used As Nanoreactor for Helix-Sense-Selective Polymerization. *ACS Macro Letters* **2017,** *6*, 6-10.
(19) Zhou, L.; Chu, B.-F.; Xu, X.-Y.; Xu, L.; Liu, N.; Wu, Z.-Q., Significant Improvement on Enantioselectivity and Diastereoselectivity of Organocatalyzed Asymmetric Aldol Reaction Using Helical Polyisocyanides Bearing Proline Pendants. *ACS Macro Letters* **2017,** *6*, 824-829.
(20) Caillol, S.; Lecommandoux, S.; Mingotaud, A.-F.; Schappacher, M.; Soum, A.; Bryson, N.; Meyrueix, R., Synthesis and Self-Assembly Properties of Peptide−Polylactide Block Copolymers. *Macromolecules* **2003,** *36*, 1118-1124.
(21) Rodríguez-Hernández, J.; Lecommandoux, S., Reversible Inside−Out Micellization of pH-responsive and Water-Soluble Vesicles Based on Polypeptide Diblock Copolymers. *J. Am. Chem. Soc.* **2005,** *127*, 2026-2027.
(22) Schatz, C.; Louguet, S.; Le Meins, J.-F.; Lecommandoux, S., Polysaccharide-block-polypeptide Copolymer Vesicles: Towards Synthetic Viral Capsids. *Angewandte Chemie International Edition* **2009,** *48*, 2572-2575.
(23) Yamashita, H.; Misawa, T.; Oba, M.; Tanaka, M.; Naito, M.; Kurihara, M.; Demizu, Y., Development of helix-stabilized cell-penetrating peptides containing cationic α,α-disubstituted amino acids as helical promoters. *Bioorganic & Medicinal Chemistry* **2017,** *25*, 1846-1851.
(24) Chen, Y.; Zhang, Z.-H.; Han, X.; Yin, J.; Wu, Z.-Q., Oxidation and Acid Milieu-Disintegratable Nanovectors with Rapid Cell-Penetrating Helical Polymer Chains for Programmed Drug Release and Synergistic Chemo-Photothermal Therapy. *Macromolecules* **2016,** *49*, 7718-7727.
(25) Zhang, W.-M.; Zhang, J.; Qiao, Z.; Liu, H.-Y.; Wu, Z.-Q.; Yin, J., Facile Fabrication of Positively-Charged Helical Poly(phenyl isocyanide)s Modified Multi-Stimuli-Responsive Nanoassembly Capable of High Efficiency Cell-Penetrating, Ratiometric Fluorescence Imaging, and Rapid Intracellular Drug Release. *Polym. Chem.* **2018,** *9*, 4233-4242
(26) Penfold, N. J. W.; Yeow, J.; Boyer, C.; Armes, S. P., Emerging Trends in Polymerization-Induced Self-Assembly. *ACS Macro Letters* **2019,** *8*, 1029-1054.
(27) Warren, N. J.; Armes, S. P., Polymerization-Induced Self-Assembly of Block Copolymer Nano-objects via RAFT Aqueous Dispersion Polymerization. *J. Am. Chem. Soc.* **2014,** *136*, 10174-10185.
(28) Cunningham, V. J.; Alswieleh, A. M.; Thompson, K. L.; Williams, M.; Leggett, G. J.; Armes, S. P.; Musa, O. M., Poly(glycerol monomethacrylate)–Poly(benzyl methacrylate) Diblock Copolymer Nanoparticles via RAFT Emulsion Polymerization: Synthesis, Characterization, and Interfacial Activity. *Macromolecules* **2014,** *47*, 5613-5623.
(29) Derry, M. J.; Fielding, L. A.; Armes, S. P., Industrially-relevant polymerization-induced self-assembly formulations in non-polar solvents: RAFT dispersion polymerization of benzyl methacrylate. *Polym. Chem.* **2015,** *6*, 3054-3062.
(30) Foster, J. C.; Varlas, S.; Couturaud, B.; Jones, J. R.; Keogh, R.; Mathers, R. T.; O'Reilly, R. K., Predicting Monomers for Use in Polymerization-Induced Self-Assembly. *Angewandte Chemie International Edition* **2018,** *57*, 15733-15737.
(31) Lecommandoux, S.; Grazon, C.; Salas-Ambrosio, P.; Ibarboure, E.; Buol, A.; Garanger, E.; Grinstaff, M. W.; Bonduelle, C., Aqueous Ring-Opening Polymerization-Induced Self-Assembly (ROPISA) of N-carboxyanhydrides. *Angewandte Chemie International Edition* **2019**, doi:10.1002/anie.201912028.
(32) Kapishon, V.; Whitney, R. A.; Champagne, P.; Cunningham, M. F.; Neufeld, R. J., Polymerization Induced Self-Assembly of Alginate Based Amphiphilic Graft Copolymers Synthesized by Single Electron Transfer Living Radical Polymerization. *Biomacromolecules* **2015,** *16*, 2040-2048.
(33) Okubo, M.; Sugihara, Y.; Kitayama, Y.; Kagawa, Y.; Minami, H., Emulsifier-Free, Organotellurium-Mediated Living Radical Emulsion Polymerization of Butyl Acrylate. *Macromolecules* **2009,** *42*, 1979-1984.
(34) Cordella, D.; Ouhib, F.; Aqil, A.; Defize, T.; Jérôme, C.; Serghei, A.; Drockenmuller, E.; Aissou, K.; Taton, D.; Detrembleur, C., Fluorinated Poly(ionic liquid) Diblock Copolymers Obtained by Cobalt-Mediated Radical Polymerization-Induced Self-Assembly. *ACS Macro Letters* **2017,** *6*, 121-126.
(35) Ferguson, C. J.; Hughes, R. J.; Pham, B. T. T.; Hawkett, B. S.; Gilbert, R. G.; Serelis, A. K.; Such, C. H., Effective ab Initio Emulsion Polymerization under RAFT Control. *Macromolecules* **2002,** *35*, 9243-9245.
(36) Wan, W.-M.; Pan, C.-Y., Atom Transfer Radical Dispersion Polymerization in an Ethanol/Water Mixture. *Macromolecules* **2007,** *40*, 8897-8905.
(37) Canning, S. L.; Smith, G. N.; Armes, S. P., A Critical Appraisal of RAFT-Mediated Polymerization-Induced Self-Assembly. *Macromolecules* **2016,** *49*, 1985-2001.

(38) Kim, K. H.; Kim, J.; Jo, W. H., Preparation of hydrogel nanoparticles by atom transfer radical polymerization of N-isopropylacrylamide in aqueous media using PEG macro-initiator. *Polymer* **2005,** *46*, 2836-2840.
(39) Guégain, E.; Zhu, C.; Giovanardi, E.; Nicolas, J., Radical Ring-Opening Copolymerization-Induced Self-Assembly (rROPISA). *Macromolecules* **2019,** *52*, 3612-3624.
(40) Zhang, L.; Song, C.; Yu, J.; Yang, D.; Xie, M., One-pot synthesis of polymeric nanoparticle by ring-opening metathesis polymerization. *Journal of Polymer Science Part A: Polymer Chemistry* **2010,** *48*, 5231-5238.
(41) Wright, D. B.; Touve, M. A.; Adamiak, L.; Gianneschi, N. C., ROMPISA: Ring-Opening Metathesis Polymerization-Induced Self-Assembly. *ACS Macro Letters* **2017,** *6*, 925-929.
(42) Foster, J. C.; Varlas, S.; Blackman, L. D.; Arkinstall, L. A.; O'Reilly, R. K., Ring-Opening Metathesis Polymerization in Aqueous Media Using a Macroinitiator Approach. *Angewandte Chemie International Edition* **2018,** *57*, 10672-10676.
(43) Varlas, S.; Foster, J. C.; O'Reilly, R. K., Ring-opening metathesis polymerization-induced self-assembly (ROMPISA). *Chemical Communications* **2019,** *55*, 9066-9071.
(44) Blackman, L. D.; Varlas, S.; Arno, M. C.; Fayter, A.; Gibson, M. I.; O'Reilly, R. K., Permeable Protein-Loaded Polymersome Cascade Nanoreactors by Polymerization-Induced Self-Assembly. *ACS Macro Letters* **2017,** *6*, 1263-1267.
(45) Blackman, L. D.; Varlas, S.; Arno, M. C.; Houston, Z. H.; Fletcher, N. L.; Thurecht, K. J.; Hasan, M.; Gibson, M. I.; O'Reilly, R. K., Confinement of Therapeutic Enzymes in Selectively Permeable Polymer Vesicles by Polymerization-Induced Self-Assembly (PISA) Reduces Antibody Binding and Proteolytic Susceptibility. *ACS Central Science* **2018,** *4*, 718-723.
(46) Asaoka, S.; Joza, A.; Minagawa, S.; Song, L.; Suzuki, Y.; Iyoda, T., Fast Controlled Living Polymerization of Arylisocyanide Initiated by Aromatic Nucleophile Adduct of Nickel Isocyanide Complex. *ACS Macro Letters* **2013,** *2*, 906-911.
(47) Takei, F.; Yanai, K.; Onitsuka, K.; Takahashi, S., Screw-Sense-Selective Polymerization of Aryl Isocyanides Initiated by a Pd-Pt μ-Ethynediyl Dinuclear Complex: A Novel Method for the Synthesis of Single-Handed Helical Poly(isocyanide)s with the Block Copolymerization Technique. *Chem. Eur. J.* **2000,** *6*, 983-993.
(48) Lee, J.; Shin, S.; Choi, T.-L., Fast Living Polymerization of Challenging Aryl Isocyanides Using an Air-Stable Bisphosphine-Chelated Nickel(II) Initiator. *Macromolecules* **2018,** *51*, 7800-7806.
(49) Han, J.; You, J.; Li, X.; Duan, P.; Liu, M., Full-Color Tunable Circularly Polarized Luminescent Nanoassemblies of Achiral AIEgens in Confined Chiral Nanotubes. *Adv Mater* **2017,** *29*, 1606503.
(50) Okazaki, Y.; Goto, T.; Sakaguchi, R.; Kuwahara, Y.; Takafuji, M.; Oda, R.; Ihara, H., Facile and Versatile Approach for Generating Circularly Polarized Luminescence by Non-chiral, Low-molecular Dye-on-nanotemplate Composite System. *Chem. Lett.* **2016,** *45*, 448-450.
(51) Li, H.; Zheng, X.; Su, H.; Lam, J. W. Y.; Sing Wong, K.; Xue, S.; Huang, X.; Huang, X.; Li, B. S.; Tang, B. Z., Synthesis, optical properties, and helical self-assembly of a bivaline-containing tetraphenylethene. *Scientific Reports* **2016,** *6*, 19277.
(52) Liu, M.; Zhang, L.; Wang, T., Supramolecular Chirality in Self-Assembled Systems. *Chem Rev* **2015,** *115*, 7304-97.